LETTER **Communicated by Daniel Wolpert**

Different Predictions by the Minimum Variance and Minimum Torque-Change Models on the Skewness of Movement Velocity Profiles

Hirokazu Tanaka
Center for Neurobiology and Behavior and Department of Physiology and Cellular Biophysics, Columbia University, New York, NY 10032, U.S.A.

Meihua Tai
Department of Mechanical Engineering, Polytechnic University, Brooklyn, NY 11201, U.S.A.

Ning Qian
nq6@columbia.edu
Center for Neurobiology and Behavior and Department of Physiology and Cellular Biophysics, Columbia University, New York, NY 10032, U.S.A.

We investigated the differences between two well-known optimization principles for understanding movement planning: the minimum variance (MV) model of Harris and Wolpert (1998) and the minimum torque change (MTC) model of Uno, Kawato, and Suzuki (1989). Both models accurately describe the properties of human reaching movements in ordinary situations (e.g., nearly straight paths and bell-shaped velocity profiles). However, we found that the two models can make very different predictions when external forces are applied or when the movement duration is increased. We considered a second-order linear system for the motor plant that has been used previously to simulate eye movements and single-joint arm movements and were able to derive analytical solutions based on the MV and MTC assumptions. With the linear plant, the MTC model predicts that the movement velocity profile should always be symmetrical, independent of the external forces and movement duration. In contrast, the MV model strongly depends on the movement duration and the system's degree of stability; the latter in turn depends on the total forces. The MV model thus predicts a skewed velocity profile under many circumstances. For example, it predicts that the peak location should be skewed toward the end of the movement when the movement duration is increased in the absence of any elastic force. It also predicts that with appropriate viscous and elastic forces applied to increase system stability, the velocity profile should be skewed toward the beginning of the movement. The velocity profiles predicted by the MV model can even show oscillations when the plant becomes highly oscillatory. Our

analytical and simulation results suggest specific experiments for testing the validity of the two models.

1 Introduction

The problem of motor planning is ill posed. For a given initial and a target position, the required control signals cannot be uniquely determined (Bernstein, 1967). Conceptually, the problem can be divided into a few subproblems (Hollerbach, 1982; Kawato, Furukawa, & Suzuki, 1987): (1) the determination of a desired trajectory given an initial and a target position in the visual coordinate system, (2) the coordinate transformation of the trajectory from the visual coordinate system to the body-oriented coordinate system, (3) the determination of muscle torques for producing the desired trajectory, and (4) the specification of neuronal control signals for realizing the muscle torques. In general, each of these subproblems is ill posed due to kinematic or dynamic redundancies.

To understand why the brain chooses a particular motor plan among infinite possibilities, it is usually assumed that the motor system tries to optimize a certain quantity related to movements. One such optimization principle is the minimum jerk (MJ) model proposed by Flash and Hogan (1985). The model determines a unique trajectory by minimizing jerk, the third temporal derivation of trajectory in the task-oriented coordinate system. It thus prefers paths with smooth acceleration. It predicts straight paths and bell-shaped velocity profiles often observed in human reaching movements. The MJ model is purely kinematic, and it provides a solution to the first subproblem mentioned above. Later, dynamic models were also proposed, attempting to solve more than one subproblem simultaneously. We will analyze and compare two representative dynamic models in this article: the minimum torque change (MTC) model (Uno, Kawato, & Suzuki, 1989) and the minimum variance (MV) model (Harris & Wolpert, 1998). The MTC model is a dynamical extension of the MJ model; it prefers smooth muscle torques instead of acceleration. In contrast, the MV model introduces a signal-dependent noise term into the control signals and requires a minimum postmovement variance around the target position. These dynamic models explain a wider range of experimental observations than the MJ model does (Uno, Kawato, et al., 1998; Harris & Wolpert, 1998). Several authors have discussed how these optimization processes may be implemented in a biologically plausible network (Massone & Bizzi, 1989; Kawato, Maede, Uno, & Suzuki, 1990; Hoff & Arbib, 1993).

The MTC and MV models make similar predictions for movements under normal situations (Uno, Kawato, & Suzuki, 1989; Harris & Wolpert, 1998), such as nearly straight paths and bell-shaped velocity profiles (Kelso, Southard, & Goodman, 1979; Morasso, 1981; Abend, Bizzi, & Morasso, 1982). This is remarkable since the two models employ very different optimization criteria: the MTC model prefers the smoothness of muscle torques during

the movement, while the MV model focuses on the accuracy after the movement. The main purpose of this article is to explore the conditions under which the two models make divergent predictions. Obviously, this is important for determining which optimization principle, if any, may be used by the brain for motor planning. Specifically, we formulate these optimization processes with a linear motor plant and show that the velocity profiles predicted by the MV model can be highly asymmetrical when we change the movement duration or the balance between viscous and elastic forces, while the MTC model always predicts a symmetrical velocity profile. In section 2, we provide an analytical formulation of these two models with a linear plant and explain the underlying reasons for the different predictions. We also determine the conditions under which the velocity profiles predicted by the MV model become skewed toward the beginning or the end of a movement. In section 3, we verify our analyses with numerical simulations of representative cases. We discuss in section 4 some specific experiments for testing the models. Since neither model includes sensory feedback, we also briefly discuss potential effects of feedback on the velocity profile in the framework of Todorov and Jordan's recent model (Todorov & Jordan, 2002; Todorov, 2004). Preliminary results have been presented in abstract form (Tanaka & Qian, 2003).

2 Analyses

Let us first define a motor plant to be used by both the MTC and the MV models. We consider a second-order linear system whose dynamics is specified by

$$\ddot{\theta}(t) + a_1\dot{\theta}(t) + a_0\theta(t) = \tau(t). \tag{2.1}$$

This equation is based on Newtonian mechanics and has been used for modeling eye movements (Robinson, Gordon, & Gordon, 1986) and single-joint arm movements (Hogan, 1984). (The nonlinear equations for a two-joint arm (Luh, Walker, & Paul, 1980) reduce to this linear form when the upper joint is assumed to be fixed.) Here, a_0 and a_1 are elastic and viscous constants, respectively. θ is a state variable representing eye position or joint angle, and a dot over the variable denotes the temporal derivative. $\tau(t)$ is the muscle torque. In our analysis of the MV model, we will make the simplifying assumption that τ is also the neural control signal. In other words, we assume that there is no delay between neural activity and muscle responses. This simplification allows us to use the same dynamic equation for the MTC and MV models and derive analytical solutions. In reality, the muscle torque should be a low-pass filtered version of the control signal (Winters & Stark, 1985). We will introduce this more realistic relationship in our numerical simulations in section 3, and show that it does not change the conclusions of our analysis.

The second-order differential equation 2.1 can be reduced to the first order by introducing a vector representation of the state:

$$x \equiv \begin{pmatrix} \theta \\ \dot{\theta} \end{pmatrix}. \tag{2.2}$$

Then the equation becomes

$$\dot{x}(t) = Ax(t) + B\tau(t), \tag{2.3}$$

where the matrices A and B are defined as

$$A \equiv \begin{pmatrix} 0 & 1 \\ -a_0 & -a_1 \end{pmatrix}, \qquad B \equiv \begin{pmatrix} 0 \\ 1 \end{pmatrix}. \tag{2.4}$$

The stability of the plant is determined by the eigenvalues of the matrix A,

$$\lambda_{\pm} = \left(-a_1 \pm \sqrt{a_1^2 - 4a_0} \right) /2. \tag{2.5}$$

The system is stable if the real parts of both eigenvalues are negative, and unstable otherwise. This stability condition is satisfied if both a_0 and a_1 are positive. The stable system is called over-, critical-, or underdamped according to whether $a_1^2 > 4a_0$, $a_1^2 = 4a_0$, or $a_1^2 < 4a_0$, respectively. We can control the system's degree of stability by adjusting a_0 and a_1 to alter the real-part magnitude of the eigenvalues $\lambda_{\pm}$. The system can also be made oscillatory (underdamped) by increasing the elastic force relative to the viscous force.

Equation 2.3 can be integrated after a coordinate transform that diagonalizes A, and $\theta(t)$ and $\dot{\theta}(t)$ can then be obtained via the inverse transform. The results are:

$$\theta(t) = \frac{(\lambda_+ e^{\lambda_- t} - \lambda_- e^{\lambda_+ t})\theta_0 + \int_0^t \left(e^{\lambda_+(t-t')} - e^{\lambda_-(t-t')} \right) \tau(t') dt'}{(\lambda_+ - \lambda_-)} \tag{2.6}$$

$$\dot{\theta}(t) = \frac{\lambda_+\lambda_-(-e^{\lambda_+ t} + e^{\lambda_- t})\theta_0 + \int_0^t \left(\lambda_+ e^{\lambda_+(t-t')} - \lambda_- e^{\lambda_-(t-t')} \right) \tau(t') dt'}{(\lambda_+ - \lambda_-)} \tag{2.7}$$

under the initial condition that $\theta(0) = \theta_0$ and $\dot{\theta}(0) = 0$. Thus, $\theta(t)$ and $\dot{\theta}(t)$ are essentially filtered versions of $\tau(t)$. Equation 2.7 will be used in our numerical simulations of the MTC model's velocity profiles in section 3.

2.1 The Minimum Torque-Change Model. We show analytically that with the second-order linear plant, the MTC model always predicts symmetrical velocity profiles of movement.

2.1.1 The Cost Function. The cost function of the MTC model is defined as an integration of the torque changes over the movement duration $[0, t_f]$ (Uno, Kawato, et al., 1998),

$$C_{MTC} = \frac{1}{2}\int_0^{t_f} \dot{\tau}^2(t)dt. \tag{2.8}$$

If there are no elastic and viscous forces in equation 2.1, this cost function reduces to that for the MJ model. By minimizing the cost function, a unique trajectory is specified among all trajectories that satisfy equation 2.1 and appropriate boundary conditions (see below). The optimization process can be solved by using either the Lagrange multiplier method (Uno, Kawato, et al., 1989) or the Euler-Lagrange equation (Wada, Kaneko, Nakano, Osu, & Kawato, 2001). The latter method is more convenient for proving the symmetry of the velocity profile, as we show below. The solution based on the Lagrange multiplier method is provided in the appendix and is used in our numerical simulations in section 3.

2.1.2 Symmetric Velocity Profiles Predicted by the MTC Model. By substituting equation 2.1 into equation 2.8 and applying the variational procedure with respect to θ, we obtain the following Euler-Lagrange equation (Wada et al., 2001):

$$\frac{d^6\theta(t)}{dt^6} - a_1^2\frac{d^4\theta(t)}{dt^4} + a_0^2\frac{d^2\theta(t)}{dt^2} = 0. \tag{2.9}$$

The boundary terms of the partial integrations vanish because of the zero velocity and acceleration conditions at the initial and final times. This equation is clearly invariant under time translation. We can thus let the movement duration be from $-t_f/2$ to $t_f/2$ such that a symmetrical velocity profile is equivalent to an even function of time. The boundary conditions are $\theta(-t_f/2) = \theta_0$, $\theta(t_f/2) = \theta_f$, and $\dot{\theta}(-t_f/2) = \dot{\theta}(t_f/2) = \ddot{\theta}(-t_f/2) = \ddot{\theta}(t_f/2) = 0$.

The above differential equation is reduced to fifth order if we use the velocity $\omega(t) \equiv \dot{\theta}(t)$ as the variable

$$\frac{d^5\omega(t)}{dt^5} - a_1^2\frac{d^3\omega(t)}{dt^3} + a_0^2\frac{d\omega(t)}{dt} = 0, \tag{2.10}$$

and the original boundary conditions become five new conditions: $\omega(-t_f/2) = \omega(t_f/2) = \dot{\omega}(-t_f/2) = \dot{\omega}(t_f/2) = 0$, and $\int_{-t_f/2}^{t_f/2} dt\omega(t) = \theta_f - \theta_0$. The eigenvalues of equation 2.10 are zero and four nonzero values α_i $(i = 1, 2, 3, 4)$ given by the characteristic polynomial:

$$\alpha^4 - a_1^2\alpha^2 + a_0^2 = 0. \tag{2.11}$$

The solution of equation 2.10 is a linear combination of the eigenstates, $\omega(t) = \beta_0 + \sum_{i=1}^{4} \beta_i e^{\alpha_i t}$ where the coefficients β_i are determined by the five conditions mentioned above. Since equation 2.11 is a function of α^2, only two of the four eigenvalues, say α_1 and α_3, are independent, and the other two are given by $\alpha_2 = -\alpha_1$ and $\alpha_4 = -\alpha_3$. It is then straightforward, though tedious, to solve for β_i and show that they satisfy the following simple relations:

$$\beta_1 = \beta_2, \qquad \beta_3 = \beta_4. \tag{2.12}$$

Using this result, the velocity can be expressed as

$$\omega(t) = \beta_0 + \beta_1 \left(e^{\alpha_1 t} + e^{-\alpha_1 t}\right) + \beta_3 \left(e^{\alpha_3 t} + e^{-\alpha_3 t}\right). \tag{2.13}$$

This solution is an even function of time $\omega(-t) = \omega(t)$. Therefore, with the linear plant, the velocity profile predicted by the MTC model is always exactly symmetrical regardless of the parameter values.

2.2 The Minimum Variance Model. We now consider the MV model with the second-order linear plant and determine the conditions under which the velocity profiles are asymmetrical.

2.2.1 The Cost Function. According to the MV model (Harris & Wolpert, 1998), a signal-dependent noise term ξ should be added to the dynamic equation 2.3:

$$\dot{x}(t) = Ax(t) + B\left[\tau(t) + \xi(t)\right]. \tag{2.14}$$

ξ is assumed to be a gaussian white noise with zero mean and a variance proportional to the square of the control signal τ (Harris & Wolpert, 1998):

$$\mathrm{E}[\xi(t)] = 0, \quad \mathrm{E}[\xi(t)\xi(t')] = K\tau^2(t)\delta(t - t'). \tag{2.15}$$

Here K is a proportionality constant that scales the amplitude of noise. $\mathrm{E}[\cdot]$ denotes the operation of taking an average over the noise distribution.

The dynamic equation 2.14 is stochastic, so it is not particularly informative to consider each individual trajectory. Instead, we consider the expected value of the state vector and the covariance matrix by averaging over the signal-dependent noise ξ:

$$\mathrm{E}[x(t)] = e^{At}x_0 + \int_0^t e^{A(t-t')}B\tau(t')dt', \tag{2.16}$$

$$\mathrm{Cov}[x(t)] = K\int_0^t e^{A(t-t')}B\left(e^{A(t-t')}B\right)^T \tau^2(t')dt'. \tag{2.17}$$

Here $x_0 = (\theta_0, 0)^T$ is the initial state vector at $t = 0$. These expressions are obtained by integrating the equation of motion, equation 2.14, and then taking the average over the noise variable according to equation 2.15.

Consider a movement over an interval $0 \le t \le t_f$. The cost function to be minimized by the MV model is the variance of the position summed over a certain postmovement duration $[t_f, t_f + t_p]$ (Harris & Wolpert, 1998). We first consider the simplified case that the cost function is the variance of the position at the final time point t_f only. The problem, then, is to minimize the variance of position θ at t_f under the constraint that the expected value of the state x at t_f is the target state $x_f = (\theta_f, 0)^T$ (Harris & Wolpert, 1998). The variance of the position is the (1,1) component of the 2×2 covariance matrix, equation 2.17. The constrained optimization can be solved by introducing a 2×1 Lagrange multiplier μ, with the resulting augmented cost function:

$$C'_{MV} = K \int_0^{t_f} f(t; t_f)\, \tau^2(t)\, dt - \mu^T \left(E[x(t_f)] - x_f \right), \tag{2.18}$$

where

$$f(t; t_f) \equiv \left[e^{A(t_f - t)} B (e^{A(t_f - t)} B)^T \right]_{1,1}. \tag{2.19}$$

The subscript denotes the $(1, 1)$ component of the matrix. $f(t; t_f)$ is a weighting factor that determines how much the noise in control signal $\tau(t)$ at time t contributes to the final variance of position. By applying the variational principle with respect to $\tau(t)$ to equation 2.18, we obtain an analytical solution for the optimal control signal:

$$\tau(t) = \frac{\mu^T e^{A(t_f - t)} B}{2K f(t; t_f)}. \tag{2.20}$$

The Lagrange multiplier vector μ is a constant that can be determined via equation 2.16 and the boundary condition $\mathrm{E}[x(t_f)] = x_f$. Note that the control signal $u(t)$ is inversely related to the weighting factor $f(t; t_f)$. This makes sense because, as we mentioned above, $f(t; t_f)$ determines how much the noise in the control signal at time t will contribute to the variance at the final time t_f. A large f means a large contribution, and the corresponding noise (and thus the control signal) should be small in order to minimize the final variance.

A problem with the above simplification is that since $f(t_f; t_f) = 0$ according to equation 2.19, $u(t)$ given by equation 2.20 diverges at t_f. The problem can be avoided by using the integration of the variance (and also the constraint) over a postmovement period $[t_f, t_f + t_p]$ as the cost function (Harris & Wolpert, 1998). The reason is that noise at t_f does not affect positional variance at t_f but does contribute to the variance after t_f. It can then be

shown that equation 2.20 becomes

$$\tau(t) = \frac{\int_{t_f}^{t_f+t_p} \mu(t')^T e^{At'} dt' e^{-At} B}{2K \int_{t_f}^{t_f+t_p} f(t; t') dt'} \qquad (0 \le t \le t_f) \tag{2.21}$$

$$\tau(t) = a_0 \theta_f \qquad (t_f < t \le t_f + t_p), \tag{2.22}$$

and the divergence problem disappears. Here, the Lagrange multiplier vector $\mu(t)$ is a function of time. The meaning of equation 2.21 is similar to that of equation 2.20, with the torque inversely proportional to the weighting factor for the noise. Equation 2.22 is the torque needed for balancing the elastic force over the postmovement period in order to keep the position at θ_f.

2.2.2 Velocity Profiles Predicted by the MV Model. A precise discussion of the velocity profile shape predicted by the MV mode requires determining the Lagrange multiplier vector μ from the boundary conditions and then substituting equation 2.20 into equation 2.7. However, since the result will be complicated, involving integrals with no closed-form solutions, we take a more heuristic approach here and verify our conclusions via numerical simulations in section 3. Specifically, we focus on the weighting factor $f(t; t_f)$ because it determines how much the noise in the control signal $\tau(t)$ at time t contributes to the positional variance at the end of the movement t_f. If, for example, $f(t; t_f)$ is small at the start of a movement and becomes large near the end, then the signal-dependent noise during the early phase of the movement does not matter as much as the noise near the end, and we expect a large initial control signal and a velocity profile skewed toward the beginning.

Using the same diagonalization procedure for obtaining equation 2.7, we can express the weighting factor, equation 2.19, in terms of the two eigenvalues $\lambda_\pm$ of matrix A. For the nondegenerate case $\lambda_+ \neq \lambda_-$, the weighting factor is given by

$$f(t; t_f) = \frac{\left(e^{\lambda_+(t_f-t)} - e^{\lambda_-(t_f-t)}\right)^2}{(\lambda_+ - \lambda_-)^2} \qquad (0 \le t \le t_f), \tag{2.23}$$

and for the degenerate (i.e., critical damping) case where the two eigenvalues $\lambda_\pm$ take the same value λ,

$$f(t; t_f) = (t_f - t)^2 \, e^{2\lambda(t_f-t)} \qquad (0 \le t \le t_f). \tag{2.24}$$

We first consider a stable case when both eigenvalues are real and negative. By differentiating equations 2.23 and 2.24, the weighting factor is found to have a single peak at

$$t^* = t_f - \frac{1}{\lambda_+ - \lambda_-} \ln \frac{\lambda_-}{\lambda_+} \tag{2.25}$$

for the nondegenerate plant and

$$t^* = t_f + \frac{1}{\lambda} \tag{2.26}$$

for the degenerate plant. For real and negative eigenvalues, we have $|\lambda_-| \geq |\lambda_+|$ according to equation 2.5, and it is easy to see that t^* is always less than t_f. The system is most stable when the two negative eigenvalues have similar and large magnitudes. Under this condition, t^* is very close to t_f, indicating that noise in the early phase of movement tends to decay away quickly and does not contribute much to the final variance. This means that the control signal can be large around the start of the movement, and the velocity profile should thus be skewed toward the movement onset. As one or both eigenvalues become smaller in magnitude, the system's degree of stability decreases, and t^* shifts toward the start of the movement. (With very small eigenvalue magnitudes, t^* can even be less than 0, and the weighting factor will be a monotonically deceasing function over $[0, t_f]$.) Consequently, the early noise becomes more and more important, the control signal should thus be weaker near the movement onset, and the velocity profile will eventually become more skewed toward the end of the movement.

Next, we consider the unstable case where the eigenvalues are real but at least one of them is positive. This implies a negative viscous constant, which could be realized with a robotic manipulandum. In this case, it can be shown that the weighting factor, equation 2.23 or equation 2.24, is a monotonically decreasing function of time. Again, this means that the velocity profile should be skewed toward the end of the movement.

In the case of complex eigenvalues $\lambda_\pm = \mu \pm i\nu$, the system is oscillatory. The analytical expression for the weighting factor becomes

$$f(t; t_f) = \frac{e^{2\mu(t_f - t)}}{2\nu^2}\left[1 - \cos 2\nu(t_f - t)\right], \tag{2.27}$$

which is also oscillatory with frequency ν/π. When this frequency is sufficiently high, one expects to see oscillation in the control signal and thus in the velocity profile as well.

We plot in Figure 1 the weighting factor as a function of time for a few representative cases. Figure 1A shows curves corresponding to four negative eigenvalues for the degenerate (critical damping) plant. As mentioned above, the peak shifts to the left as the system's degree of stability (the magnitude of the eigenvalue) decreases. A stable overdamping, an unstable, and a stable underdamping (oscillatory) case are shown in Figure 1B.

Finally, since the above arguments are based on how the signal-dependent noise propagates through time, one expects that the movement duration should affect the shape of the velocity profile in the MV model. For a very stable system where the noise decays with time, a longer duration

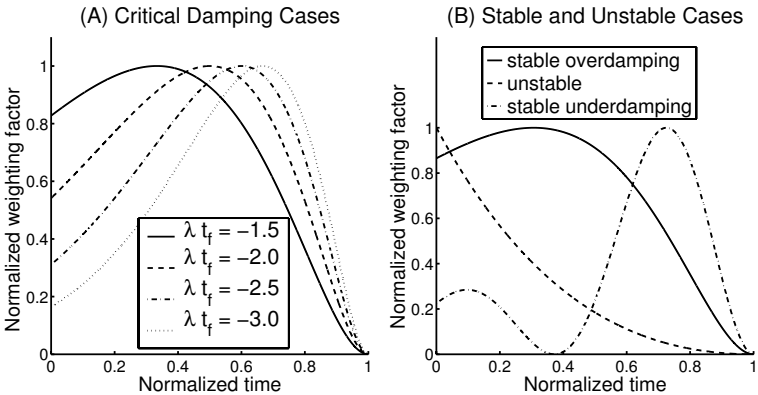

Figure 1: The weighting factor $f(t; t_f)$ plotted as a function of normalized time t/t_f. (A) Four cases of stable, critical damping with λt_f equal to -1.5, -2.0, -2.5, and -3.0 from left to right. (B) A stable overdamping ($\lambda_{\pm} t_f = -1, -2$), an unstable ($\lambda_{\pm} t_f = 0.4, 0.2$), and a stable underdamping (oscillatory) case ($\lambda_{\pm} t_f = -1 \pm 5i$).

will make the early noise contribute even less to the final variance, and the velocity profile should be skewed more toward the movement onset with increasing duration. This explains a result in Harris and Wolpert (1998) that the velocity profile of a saccadic eye movement model becomes more skewed toward the beginning with longer duration. Likewise, if the system is less stable or unstable such that the velocity profile is skewed toward the end, the skewing can be slight for a short duration but should become more pronounced with increasing duration.

Note that duration is a prefixed parameter in both the MV and MTC models that does not depend on movement amplitude, even though actual movement duration usually increases with amplitude (Fitts, 1954). For the linear plant we used, both models predict that when the movement amplitude is changed, the velocity profile will simply be scaled up or down without changing its duration or shape. One can avoid this problem by an ad hoc adjustment of the movement duration according to the amplitude prior to the optimization procedure.

We summarize our arguments for the MV model as follows. When we change the viscous and elastic constants of the system by applying external viscous and elastic forces, the shape of the movement velocity profiles should change. In particular, when the system is made more (or less) stable, the peak of the velocity profile should be shifted toward the beginning (or end) of the movement. The skewing should be more pronounced with increasing duration. Intuitively, a more stable system tends to attenuate the signal-dependent noise more over time, the control signal (and the associ-

ated noise) can thus afford to be large around the movement onset, and the velocity profile will consequently be skewed toward the beginning. In contrast, a less stable or unstable system may amplify noise through time, the control signal should start small, and the velocity profile will be skewed toward the end. When the system is made strongly oscillatory, the noise effect oscillates in time, and the velocity profile should also show oscillation.

3 Simulations

We have conducted extensive numerical simulations in order to confirm our analyses above, particularly when the simplifying assumptions for the MV model are removed. We consider single-joint movements of the forearm with the dynamic equation

$$I_0\ddot{\theta}(t) + (b_0 + b)\dot{\theta}(t) + (k_0 + k)L_0^2\theta(t) = \tau(t). \tag{3.1}$$

This equation can be derived by fixing the shoulder angle in the two-joint arm model examined by Uno, Kawato, et al. (1989). θ represents the elbow angle and τ is the muscle torque exerted to the elbow. I_0, b_0, k_0, and L_0 are the moment of inertia, the intrinsic viscosity, the intrinsic elasticity, and the length of the forearm, respectively, and we adopt the standard values of 0.25 $\mathrm{kg \cdot m^2}$, 0.20 $\mathrm{kg \cdot m^2/s}$, 0 N/m, and 0.35 m for these parameters (Harris & Wolpert, 1998). We also included externally applied viscosity b and elasticity k for altering the system's degree of stability and oscillation. This single-joint system does not have any kinematic redundancy but does have dynamic redundancies.

For the MTC model, we used the Lagrange multiplier method presented in the appendix to find the torque numerically and then used equation 2.7 to obtain velocity.

For the MV model, we made the simplifying assumptions in section 2 that the control signal is the muscle torque and that the skewing of velocity profile can be qualitatively understood by the weighting factor f. These limitations are removed in our simulations. We considered a second-order muscle model to relate the neural control signal u to the muscle torque τ (Winters & Stark, 1985):

$$\left(1 + t_a\frac{d}{dt}\right)\left(1 + t_e\frac{d}{dt}\right)\tau(t) = u(t), \tag{3.2}$$

where t_a and t_e are muscle activation and excitation time constants, and their values are 40 and 30 ms, respectively. This equation implies that the torque is acquired by low-pass filtering the control signal. Consequently, we expect a smooth rise of the muscle torque instead of a sudden onset. We used the original cost function of Harris and Wolpert (1998) by integrating the positional variance over a period of 400 ms after the movement

(longer postmovement duration does not alter the results), and numerically calculated the velocity profiles via quadratic programming.

We considered only stable cases in our simulations since unstable cases generate divergent movement trajectories that are difficult to test experimentally. Based on our analyses, we examined how the system's degree of stability, the movement duration, and the plant oscillation affect the shape of the predicted velocity profiles.

3.1 Effects of the System's Degree of Stability. The system has different degrees of stability when its eigenvalues have different magnitudes but the same (negative) sign. The simplest way to change the degree of stability is to apply external viscous and elastic forces to the forearm. In psychophysical experiments, arbitrary elastic and viscous forces can be introduced by a robotic manipulandum. One could also add the elastic force by attaching a spring to the hand.

The movement duration was fixed at 400 ms in all simulations. We first considered the baseline simulation with no external forces ($b = k = 0$). We then increased the viscous coefficients b from 1 to 5 in step of 1 kg $\cdot$ m^2/s. This range of viscous force can be achieved by a manipulandum (Shadmehr & Mussa-Ivaldi, 1994). We also imposed an external elastic force for each b according to $k = (b_0 + b)/4I_0L_0^2$ such that the plant was in critical damping condition. k ranged from 0.33 to 220 N/m.

Based on our analyses in section 2, the velocity profile of the MV model should skew more toward the beginning as the system becomes more stable, while the velocity profile of the MTC model should always remain symmetrical. This is confirmed by the simulations in Figure 2. Figure 2A shows the normalized velocity profiles predicted by the MV model. The right-most profile is the baseline case without any external forces, and it skews slightly toward the end of the movement. The profile gradually shifts toward the movement onset as the system's degree of stability increases with the external forces. To show the peak shift more clearly, we plot in Figure 2B the normalized peak locations of the profiles in Figure 2A as a function of the external viscosity. Along the vertical axis, 0, 0.5, and 1 indicate the beginning, midpoint, and end of the movement, respectively.

The corresponding simulations for the MTC model are shown in Figures 2C and 2D. As expected, the predicted velocity profiles are always symmetrical regardless of the external forces. The six normalized velocity profiles almost overlap each other completely.

3.2 Effects of the Movement Duration. We next simulated the effects of the movement duration on the shape of the velocity profile. We varied the duration from 200 ms to 1000 ms in steps of 200 ms while keeping all other parameters to their standard values. No external forces were applied in these simulations. The results for the MV model are shown in Figures 3A and 3B. The peak of the velocity profile shifts more toward the end of the

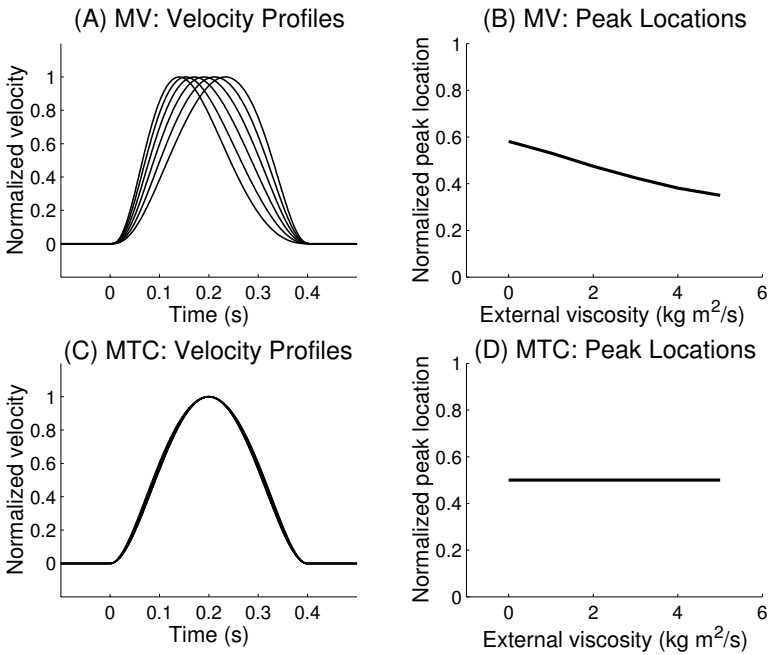

Figure 2: Velocity profiles and peak locations under different degrees of system stability. (A) Normalized velocity profiles predicted by the MV model. The rightmost curve corresponds to no external force applied to the arm model. The other four curves, from right to left, are for a critical damping system with increasing system stability via external viscous and elastic forces. (B) Normalized peak location of the velocity profiles in *A*. The peak locations are divided by the total movement duration. (C) Normalized velocity profile predicted by the MTC model with the same plant parameters as in *A*. (D) Normalized peak location of the profiles in *C*.

movement with increasing duration. In contrast, the MTC model always predicts symmetrical profile (see Figures 3C and 3D). These results are again in agreement with our analyses. The movement duration can be easily manipulated in psychophysical experiments by requiring different accuracy at the target location or varying movement amplitude (Fitts, 1954).

3.3 Effects of the Plant Oscillation. Finally, we compared the two models when the plant has complex eigenvalues and is thus oscillatory. This happens when the elastic force is more dominant over the viscous force and can be achieved by imposing a strong external elastic force or partially canceling the intrinsic viscous force via a manipulandum. In our simulations, we used the elastic coefficient k of 200, 300, and 400 N/m while keeping all

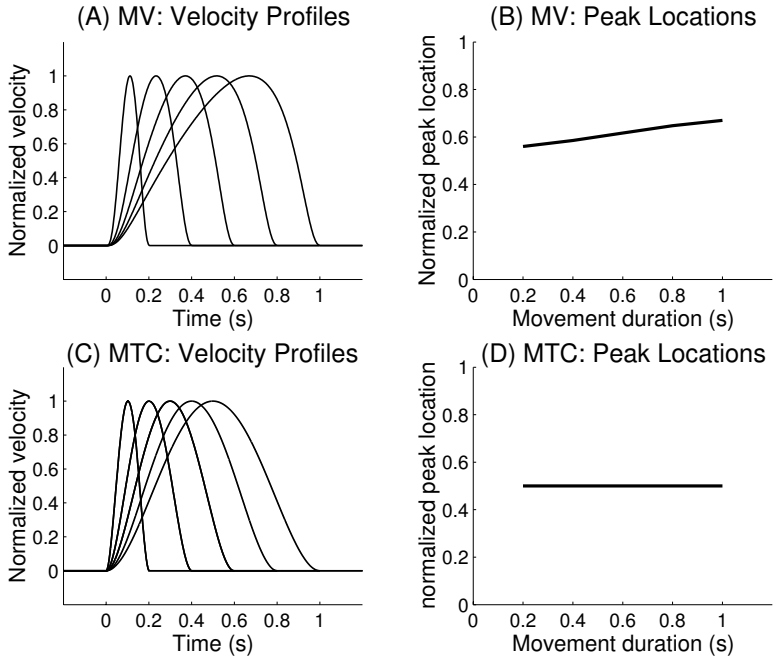

Figure 3: Velocity profiles and peak locations under various movement durations. The format is same as Figure 2, with *A* and *B* for the MV model and *C* and *D* for the MTC model.

the other parameters to their standard values. The corresponding values for vt_f/π were 1.26, 1.53, and 1.78, respectively. The movement's duration was 400 ms in all simulations.

The simulated velocity profiles for the MV model are shown in Figure 4A. The right-most curve corresponds to the largest k value. It is clear from the figure that as k increases, the profile becomes more oscillatory, and the peaks shifts toward the end of the movement. With the largest k we used, the predicted velocity is initially negative, indicating that the movement should first be in the opposite direction of the target. In contrast, the velocity profiles for the MTC model shown in Figure 4B are always symmetrical. Again, these simulations are consistent with our analytical considerations. Note that the MTC model solution, equation 2.13, can also be oscillatory when α's are complex. However, we found through simulations that k has to be larger than about 1000 N/m for the oscillation to be observed. In addition, the MTC solution always has to be symmetrical with or without oscillation.

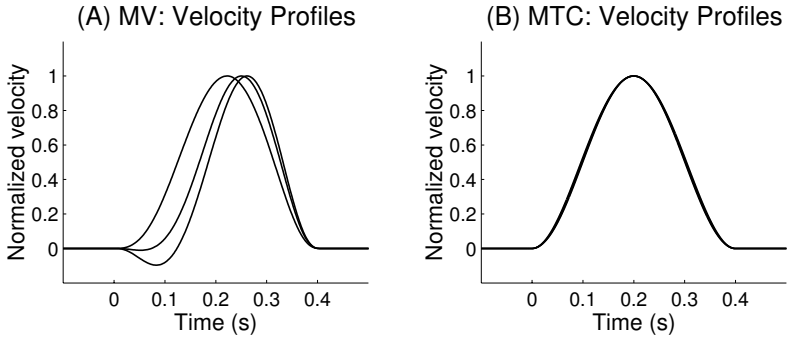

Figure 4: Velocity profiles under different degrees of plant oscillation. (A) Prediction of the MV model when the external elasticity k takes values of 200, 300, and 400 N/m, respectively. (B) Prediction of the MTC model under the same condition.

4 Discussion

The main goal of this study is to compare the two well-known models for motor planning: the minimum variance model and the minimum torque change model. We have focused on the different velocity profiles predicted by the two models and found through analyses and simulations that with a second-order linear plant, the MTC model always predicts a perfectly symmetrical velocity profile, while the MV model predicts skewed velocity profiles under many conditions. Our results suggest the following specific experiments for testing the validity of the two models. Subjects should be instructed to make single-joint movements of the forearm in a horizontal plane; this is the condition where the second-order linear plant used in our studies is valid. The movement velocity profiles should be measured under each of the following manipulations:

1. Different levels of viscous forces are applied through a manipulandum.
2. Different movement durations are imposed by asking the subjects to hit the target position with various degrees of precision.
3. Different elastic forces are applied through either a manipulandum or attachment of springs.

If the observed velocity profiles under these manipulations are all symmetrical, the MTC model is supported. But, if the velocity profiles become more skewed toward the movement onset with increasing viscosity in condition 1, the skewing is more pronounced with movement duration in condition 2, and the velocity profile becomes more skewed toward the end (and more

oscillatory) with elastic force in condition 3, the MV model is favored. All other possible outcomes will suggest that neither model is correct. In condition 1, the movement duration may increase with viscosity. This confound should not matter for testing purposes because a concurrent increase of duration with viscosity would only make the skewing predicted by the MV model stronger. When the applied elastic force is very strong in condition 3, the MV model makes the counterintuitive prediction that the movement should first be in the opposite direction of the target (see Figure 4A).

In this study, we considered the second-order linear plant that is often used in motor control modeling and can be realized with single-joint arm movements. This simplification allowed us to gain analytical insights into the two models. The simplification is justified because we are mainly interested in searching for specific conditions where the two models can be clearly differentiated. It may be desirable to extend our studies to nonlinear plants, such as the two-link arm model, because many extant experimental studies involve multijoint movements. However, nonlinear systems are not only difficult to analyze but also difficult to simulate due to the local-minimum problem in the optimization process. Our simulations (not shown) indicate that the problem becomes worse when large external forces are applied. Predictions from the two models based on nonlinear simulations may thus be less reliable for distinguishing the models than the results in this article. In addition, the MTC and MV models' predictions have a complex dependence on the system parameters in general. This makes experimental tests of the models difficult due to the uncertainties in the estimation of arm's intrinsic parameters. In contrast, we show here that for the special case of single-joint movements, the symmetry of the velocity profiles predicted by the MTC model holds for any parameter combinations. Likewise, the trend of velocity peak shift predicted by the MV model when duration and external forces are manipulated is valid regardless of the intrinsic parameter values. The simple case we considered in this article may thus provide a more conclusive test of the models.

It is known that large-amplitude saccadic eye movements show skewed velocity profiles (Collewijn, Erkelens, & Steinman, 1988; Harris & Wolpert, 1998). To the extent that the eye can be approximated by a linear plant, this observation argues against the MTC model for eye movements. Indeed, the MTC model was proposed only for arm movement, not eye movement (Uno, Kawato, et al., 1998), while the MV model was proposed for both (Harris & Wolpert, 1998). Skewed velocity profiles in arm movements have also been reported (Nagasaki, 1989; Milner & Ijaz, 1990). However, these studies usually employ multi-joint arm movements, a condition under which the MTC model can also predict skewed velocity profile (Uno, Kawato, et al., 1989). We therefore conclude that the extant data cannot distinguish the two models, and new experiments as outlined above should be performed.

Our analyses can be readily generalized to higher-order linear systems, and we expect that our conclusions will still be valid. It would also be in-

teresting to examine the implications of the other models developed by Kawato et al. that are closely related to the MTC model considered here. They include the minimum muscle-tension-change model (Uno, Suzuki, & Kawato, 1989) and the minimum motor-command-change model (Kawato, 1992). Since all of these models require smoothness in dynamic variables, and the smoothness criterion is independent of the system stability or duration, we speculate that they may all predict nearly symmetrical velocity profiles under a linear plant.

Both the MTC and MV models are purely feedforward and are perhaps most appropriate for understanding rapid, well-learned movements. However, sensory feedback, when present, has been shown to have profound effects on trajectory formation (Keele & Posner, 1968; Carlton, 1981; Sheth & Shimojo, 2002). Todorov and Jordan recently proposed an extended linear-quadratic-gaussian (LQG) model that includes sensory feedback during movement execution (Todorov & Jordan, 2002; Todorov, 2004). We have performed some simulations with their model and the linear plant used in this article, and found that sensory feedback can strongly influence the shape of the predicted velocity profile. For example, for single-joint movements without external forces, the feedback can cause the velocity profile to change from skewing toward the end to skewing toward the beginning of a movement. Since the extended LQG model contains many parameters not present in the MTC or MV model and some of those parameters (such as the relative weighting between the error and the control cost) can also influence the shape of the velocity profile, we will present a full account of the extended LQG model predictions in a future publication.

Appendix A: A Solution of the MTC Model by the Lagrange Multiplier Method

We present a solution of the MTC model based on the Lagrange multiplier method, following the original work of Uno, Kawato, et al. (1989). We used this method for our numerical simulations of the MTC model in section 3, because the Euler-Lagrange method can be numerically less stable under some parameters.

The problem is to minimize the torque change, equation 2.8, under the constraint that the dynamic equation, equation 2.3, should be satisfied. The augmented cost function after introducing a Lagrange multiplier vector p_x is thus

$$C'_{MTC} = \int_0^{t_f} dt \left(\frac{1}{2} \dot{\tau}^2 - p_x^T (\dot{x} - Ax - B\tau) \right). \tag{A.1}$$

The variation procedure would give rise to a second-order differential equation. Instead, by introducing an auxiliary variable $z(t)$ as the temporal

derivative of the torque $\tau(t)$, we obtain a new cost function,

$$\tilde{C}'_{MTC} = \int_0^{t_f} dt \left(\frac{1}{2} z^2 - p_x^T (\dot{x} - Ax - B\tau) - p_\tau (\dot{\tau} - z) \right), \tag{A.2}$$

that will give rise to a set of first-order differential equations. Here, p_τ is another Lagrange multiplier to enforce the constraint that z should be the derivative of τ. Applying the variation principle with respect to x, z, τ, p_x, and p_τ, we have the following set of equations:

$$\begin{cases} \dot{x} = Ax + B\tau, \\ z = p_T, \\ \dot{\tau} = -p_\tau, \\ \dot{p}_x = -A^T p_x, \\ \dot{p}_\tau = -B^T p_x. \end{cases} \tag{A.3}$$

The boundary conditions of the state variable at the initial and final time are

$$\begin{aligned} &\theta(0) = \theta_0, \quad \dot{\theta}(0) = 0, \quad \ddot{\theta}(0) = 0, \\ &\theta(t_f) = \theta_f, \quad \dot{\theta}(t_f) = 0, \quad \ddot{\theta}(t_f) = 0. \end{aligned} \tag{A.4}$$

The initial condition of the Lagrange multipliers $p_x(0)$ and $p_\tau(0)$ is determined so that the boundary conditions A.4 are satisfied. Finally, by integrating equations A.3, the muscle torque is obtained as

$$\tau(t) = a_0\theta_0 - p_\tau(0)t + B^T (A^T)^{-1} \left[t\mathbf{1}_2 + (A^T)^{-1} (e^{-A^T t} - \mathbf{1}_2) \right] p_x(0). \tag{A.5}$$

Here $\mathbf{1}_2$ is a 2×2 unit matrix. The optimal trajectory is obtained by solving the dynamical equation with the muscle torque, equation A.5.

Acknowledgments

We thank Emanuel Todorov and Daniel Wolpert for answering our inquiries on their models and providing us their codes. We are also grateful to John Krakauer, Pietro Mazzoni, Claude Ghez, and two anonymous reviewers for their helpful comments and suggestions. This work is supported by NIH grant MH54125.

References

Abend W., Bizzi E., & Morasso P. (1982). Human arm trajectory formation. *Brain, 105*, 331–348.

Bernstein N. (1967). The coordination and regulation of movements. London: Pergamon.

Carlton L. G. (1981). Processing visual feedback information for movement control. *Journal of Experimental Psychology: Human Perception and Performance, 7*, 1019–1030.

Collewijn H., Erkelens C. J., & Steinman R. M. (1988) Binocular coordination of human horizontal saccadic eye-movements. *Journal of Physiology*, *404*, 157–182.

Fitts P. M. (1954). Information capacity of the human motor system in controlling the amplitude of movement, *Journal of Experimental Psychology 47*, 381–391.

Flash T., & Hogan N. (1985). The coordination of movements: An experimentally confirmed mathematical model. *Journal of Neuroscience*, *5*, 1688–1703.

Harris C. M., & Wolpert D. M. (1998). Signal-dependent noise determines motor planning. *Nature*, *394*, 780–784.

Hoff B., & Arbib M. A. (1993). Models of trajectory formation and temporal information of reach and grasp. *Journal of Motor Behavior*, *25*, 175–192.

Hogan N. (1984). An organizing principle for a class of voluntary movements. *Journal of Neuroscience*, *4*, 2745–2754.

Hollerbach J. M. (1982). Computers, brains and the control of movement. *Trends in Neuroscience*, *5*, 189-192.

Kawato M. (1992). Optimization and learning in neural networks for formation and controls of coordinated movement. In D. Meyer & S. Kornlum (Eds.), *Attention and performance XIV* (pp. 821–849). Cambridge, MA: MIT Press.

Kawato M., Furukawa K., & Suzuki R. (1987). A hierarchical neural-network model for control and learning of voluntary movement. *Biological Cybernetics, 57*, 169–185.

Kawato M., Maeda Y., Uno Y., & Suzuki R. (1990). Trajectory formation of arm movement by cascade neural network model based on minimum torque-change criterion. *Biological Cybernetics*, *62*, 275–288.

Keele S. W., & Posner M. I. (1968). Processing visual feedback in rapid movements. *Journal of Experimental Psychology*, *77*, 155–158.

Kelso J. A. S., Southard D. L., & Goodman D. (1979). On the nature of human interlimb coordination. *Science*, *203*, 1029–1031.

Luh J. Y. S., Walker M. W., & Paul R. P. C. (1980). Online computational scheme for mechanical manipulators. *Journal of Dynamic Systems Measurement and Control*, *102*, 69–76.

Massone L., & Bizzi E. (1989). A neural network model for limb trajectory formation. *Biological Cybernetics, 61*, 417–425.

Milner T. E., & Ijaz M. M. (1990). The effect of accuracy constraints on 3-dimensional movement kinematics. *Neuroscience*, *35*, 365–374.

Morasso P. (1981). Spatial control of arm movements. *Experimental Brain Research, 42*, 223–227.

Nagasaki H. (1989). Asymmetric velocity and acceleration profiles of human arm movements, *Experimental Brain Research*, *74*, 319–326.

Robinson D. A., Gordon J. L., & Gordon S. E. (1986). A model of smooth pursuit eye movement system. *Biological Cybernetics*, *55*, 43–47.

Shadmehr R., & Mussa-Ivaldi F. (1994). Adaptive representation of dynamics during learning of a motor task. *Journal of Neuroscience*, *14*, 3208–3224.

Sheth B. R., & Shimojo S. (2002). How the lack of visuomotor feedback affects even the early stages of goal-directed pointing movements. *Experimental Brain Research*, *143*, 181–190.

Tanaka H., & Qian N. (2003). *Different predictions by the minimum variance and minimum torque-change models on the skewness of movement velocity profiles*. Program no. 492.7. 2003 Abstract Viewer/Itinerary Planner. Washington, DC: Society for Neuroscience. Available online at: http://sfn.scholarone.com/itin2003/index.html.

Todorov E. (2004). *Stochastic optimal control and estimation methods adapted to the noise characteristic of the sensorimotor system*. Manuscript submitted for publication.

Todorov E., & Jordan M. I. (2002). Optimality feedback control as a theory of motor coordination. *Nature Neuroscience*, *5*, 1226–1235.

Uno Y., Kawato M., & Suzuki R. (1989). Formation and control of optimal trajectory in human multijoint arm movement. *Biological Cybernetics*, *61*, 89–101.

Uno Y., Suzuki R., & Kawato M. (1989). Minimum muscle-tension-change model which reproduces human arm movement. In *Proceedings of the 4th Symposium on Biological and Physiological Engineering*, (pp. 299–302). Fukuok, Japan.

Wada Y., Kaneko Y., Nakano E., Osu R., & Kawato M. (2001). Quantitative examinations for multijoint arm trajectory planning. *Neural Networks*, *14*, 381–393.

Winters J. M., & Stark L. (1985). Analysis of fundamental human movement patterns through the use of in-depth antagonistic muscle models. *IEEE Transactions on Biomedical Engineering*, *32*, 826–839.

Received September 5, 2003; accepted April 2, 2004.